Pergamon

Insect Biochemistry and Molecular Biology 32 (2002) 1741–1756

Insect Biochemistry and Molecular Biology

www.elsevier.com/locate/ibmb

Urea and amide-based inhibitors of the juvenile hormone epoxide hydrolase of the tobacco hornworm (*Manduca sexta*: Sphingidae)

Tonya F. Severson [a], Marvin H. Goodrow [a, 1], Christophe Morisseau [a], Deanna L. Dowdy [a, 2], Bruce D. Hammock [a,*]

[a] *Department of Entomology and Cancer Research Center, University of California, Davis, CA 95616, USA*

Received 30 January 2002; received in revised form 20 June 2002; accepted 22 June 2002

Abstract

A new class of inhibitors of juvenile hormone epoxide hydrolase (JHEH) of *Manduca sexta* and further in vitro characterization of the enzyme are reported. The compounds are based on urea and amide pharmacophores that were previously demonstrated as effective inhibitors of mammalian soluble and microsomal epoxide hydrolases. The best inhibitors against JHEH activity so far within this class are N-[(Z)-9-octadecenyl]-N′-propylurea and N-hexadecyl-N′-propylurea, which inhibited hydrolysis of a surrogate substrate (*t*-DPPO) with an IC_{50} around 90 nM. The importance of substitution number and type was investigated and results indicated that N, N′-disubstitution with asymmetric alkyl groups was favored. Potencies of pharmacophores decreased as follows: amide>urea>carbamate>carbodiimide>thiourea and thiocarbamate for N, N′-disubstituted compounds with symmetric substituents, and urea>amide>carbamate for compounds with asymmetric N, N′-substituents. JHEH hydrolyzes *t*-DPPO with a K_m of 65.6 μM and a V_{max} of 59 nmol min^{-1} mg^{-1} and has a substantially lower K_m of 3.6 μM and higher V_{max} of 322 nmol min^{-1} mg^{-1} for JH III. Although none of these compounds were potent inhibitors of hydrolysis of JH III by JHEH, they are the first leads toward inhibitors of JHEH that are not potentially subject to metabolism through epoxide degradation.

Keywords: Juvenile hormone epoxide hydrolase; *Manduca sexta*; Metabolism; Inhibitors; Kinetics; Structure activity relationships (SAR); Urea; Amide; Carbamates

1. Introduction

In insects, regulation of metamorphosis is controlled by a complex interaction of endocrine agents including juvenile hormone (JH) and ecdysone (Nijhout, 1994). The level of JH present at critical times of development is regulated both by JH synthesis and by catabolism of JH (De Kort and Granger, 1981, 1996). Catabolism of JH occurs through the action of JH esterase (JHE; EC 3.1.1.1) forming JH acid, by JH epoxide hydrolase (JHEH; EC 3.3.2.3) forming JH diol, or by the alternating action of both enzymes to form the acid-diol (reviewed in Hammock, 1985). Slade and Zibitt (1971, 1972) first identified acid, diol and acid-diol metabolites of JH from the lepidopterans *Manduca sexta* and *Hyalophora cecropia*, the dipteran *Sarcophaga bullata*, and the orthopteran *Schistocerca vaga*, providing evidence for the action of both JHE and JHEH on JH in insects across several orders. Although evidence of both enzymatic activities exists across diverse insect taxa, the relative roles of the two enzymes appear to differ among insects based on the following evidence from multiple species. Metabolism of the hormone by JHE during the fifth instar is significant among lepidopterans such as *Trichoplusia ni* (Sparks and Hammock, 1980) and *M. sexta* (Sparks et al., 1983), while evidence supports the presence of greater epoxide hydrolytic activity than esterolytic activity in *M. sexta* during embryogenesis (Share et al., 1988) as well as in several dipterans such as *Musca domestica* (Hammock et al., 1977), *Drosophila*

* Corresponding author. Tel.: +1-530-752-7519; fax: +1-530-752-1537.

E-mail address: bdhammock@ucdavis.edu (B. Hammock).

[1] Present Address: 109 Almond Drive, Winters, CA 95694-2105, USA

[2] Present Address: Department of Nutrition, UC-Davis, One Shields Avenue, Davis, CA 95616, USA

0965-1748/02/$ - see front matter.
PII: S0965-1748(02)00115-7

melanogaster (Campbell et al., 1992; Casas et al., 1991b), and *Culex quinquefasciatus* (Lassiter et al., 1995). Studies using fat body and wing imaginal discs from fifth instar larvae (L5) of *M. sexta* (Hammock et al., 1975), and more recent experiments (Halarnkar and Schooley, 1990), in which significant acid-diol formation was detected after injection of newly molted fifth instar larvae with [^{3}H]-JH III, imply the presence of JHEH activity during a metamorphically significant period of development. In L5 *M. sexta*, analysis by thin layer chromatography of in vivo degradation of radiolabeled JH III indicates that two peaks of JHEH activity in tissue coincide with JHE peaks within plasma (Jesudason et al., 1992); in *T. ni* the peaks were not as tightly synchronized, with the first peak of JHE activity preceding a single broad peak of JHEH activity by one day (2nd vs 3rd day of L5) (Wing et al., 1981). Since levels of the acid and the diol (products of single hydrolytic events) were low in these assays relative to acid-diol and polar conjugates even after short exposure, it is difficult to assess whether JHE or JHEH plays a greater role in juvenile hormone clearance. In vitro kinetic assays (Touhara and Prestwich, 1993) suggest that JHEH has a greater activity upon JH than upon JH acid (higher k_{cat}/K_m), but when in vitro assays were repeated in the presence of JH binding protein (JHBP), the equilibrium shifted in favor of JHEH action upon JH acid. Several caveats must be observed, however, in evaluating these data. First, the addition of JHBP changes the amount of free substrate exposed to hydrolysis. Secondly, in the hemolymph of intact larvae—the location of JHBP—there is no appreciable JHEH activity, and little JHBP is present within tissues where JHEH is present (Hammock et al., 1975). Because conclusive evidence is lacking either for or against a role for JHEH in regulation of insect development, and because no efficient lepidopteran model exists for genomic knockouts, selective inhibitory compounds are desirable for evaluating the relative roles of JHEH and JHE in vivo. The first reports of inhibition of any epoxide hydrolase used the sterically accessible cyclodiene 3,4,5,6,8,8-hexachloro-1a,2,2a,3,6,6a,7,7a-octahydro-3,6-methanonaphth[2,3-b] oxirene (1aR,2aR,3R,6S,6aS,7aS)-rel-(9Cl) (HEOM) as a substrate (Brooks, 1973). The HEOM hydrolase of the southern armyworm, *Prodenia eridania* (now classified in genus *Spodoptera*), was shown to be inhibited by JH I, several JH mimics and glycidyl ethers (Brooks, 1973; Slade et al., 1975). Chalcone oxides (Mullin and Hammock, 1982) and glycidols (Dietze et al., 1991) were found to be potent, selective inhibitors of the mammalian soluble epoxide hydrolase and moderate inhibitors of JH III hydrolysis by the EH from *M. sexta* tissues (Casas et al., 1991a). It was later found that chalcone oxides and glycidols appear to inhibit epoxide hydrolase by being substrates that form a stable hydroxyalkyl enzyme intermediate (Morisseau et al., 1998). These inhibitors act on the mammalian soluble epoxide hydrolase in a way analogous to N-methyl carbamates inhibiting acetylcholinesterase. Linderman et al. (2000) reported a series of glycidol inhibitors with nanomolar IC_{50}s for an EH of *T. ni*. However, since these compounds contain an epoxide, one might expect that they will be substrates of EH and glutathione Stransferase, thus inhibition may be transient. Recently Morisseau et al. (1999, 2001) reported amide, urea and carbamate inhibitors of mammalian soluble and microsomal epoxide hydrolases that are EH-stable and have IC_{50}s in the low nanomolar and micromolar ranges, respectively. Because these compounds act by mimicking a transition state intermediate between the enzyme and the epoxide (Argiriadi et al., 1999, 2000; Yamada et al., 2000), and because the overall mechanism of JHEH is similar to the mammalian EH (Debernard et al., 1998; Linderman et al., 2000), one could expect that compounds with similar pharmacophores will also inhibit JHEH. In an effort to understand in greater detail the mechanism of JHEH activity and to develop tools to dissect the physiological role of the enzyme, this paper extends the biochemical characterization of recombinant *Ms*JHEH and describes the in vitro optimization of urea and amide inhibitors.

2. Materials and methods

2.1. Commercial chemicals

All chemicals and biochemical supplies used were purchased from Aldrich (Milwaukee, WI), Sigma (St Louis, MO) or Fisher Scientific (Tustin, CA) unless listed herein: dithiothreitol (Promega, Madison, WI); [^{3}H]-JH III (New England Nuclear, Boston, MA; now PE Sciences); bovine serum albumin (BSA; Fraction V) and bicinchoninic acid (BCA) assay (Pierce, Rockford, IL).

2.2. Inhibitor syntheses

The general methods for making these compounds have been described in previous papers (Argiriadi et al., 1999; Morisseau et al., 1999, 2001). In most cases the compounds were prepared by the reaction of a primary amine (or alcohol) with an alkyl- or aryl-substituted isocyanate in solvents such as hexane, ether, acetone or dimethylformamide (DMF). Products with broad melting ranges were purified by recrystallization or flash chromatography using hexane-ether or hexane-ethyl acetate gradients as eluants. Thereafter, a purity of $>$95% was evaluated by melting point within a 1–2 °C range, by thin layer chromatography when possible, using standard TLC visualization methods, and by NMR or MS. All compounds were definitively characterized by multiple spectral methods, and all analytical results supported the

proposed structures. Infrared spectra were recorded using a Galaxy Series FTIR 3000 spectrometer (Mattson Instruments, Madison, WI). ^{1}H- and/or ^{13}C-NMR spectra were obtained from a General Electric QE-300 spectrometer (Bruker NMR, Billerica, MA) operating at 300.1 and 75.5 MHz, respectively, and served to support product identity. Electrospray mass spectra were acquired on an Ultima triple-quadrupole (Micromass, Manchester, UK) using positive mode electrospray ionization (cone = 50 eV, capillary = 3.5 keV) tuned to unit resolution. A methanolic solution of each inhibitor (5 μl) was injected onto a 2.1 × 3.5 Xterra C18 column (Waters Corporation, Milford, MA) and eluted with a 5 μl min^{-1} flow of a 1:1 mixture of solvents A and B [A = 0.1% (v/v) aqueous formic acid; B = acetonitrile, 0.1% (v/v) formic acid]. Atmospheric pressure chemical ionization (APCI) mass spectra were performed using a Mariner mass spectrometer (PerSeptive Biosystems, Framingham, MA) in the positive mode (needle potential = + 5000 V).

2.3. Isolation of recombinant juvenile hormone epoxide hydrolase

Cells of *T. ni* (Hi-5) were infected in 500 ml volumes at a multiplicity of infection (plaque-forming units/cell) of 0.1–0.2 with recombinant baculovirus to express JHEH (Debernard et al., 1998). After five days, cells were harvested and centrifuged at 100***g*** for 15 min at 5 °C, and the pellet was resuspended in 20 ml of Buffer A (100 mM Tris–HCl, pH 8.0, containing 1 mM EDTA, 1 mM dithiothreitol and 1 mM phenylmethylsulfonyl fluoride). The cell suspension was homogenized using a Polytron homogenizer (Brinkmann Instruments, Westbury, NY) at setting 6 for four half-minute pulses alternating with 1–2 min of chilling on ice. Microsomal fractions were prepared as described previously, and solubilized with Buffer A containing 0.2% Triton X-100 (Debernard et al., 1998).

2.4. Substrates and protein assay

[^{3}H]-*trans*-Diphenylpropene oxide (*t*-DPPO) and unlabeled *t*-DPPO were laboratory stocks prepared by the method of Borhan et al. (1995). Radiolabeled *t*-DPPO was diluted with unlabeled *t*-DPPO in DMF to obtain a working stock of substrate having a final concentration of 5 mM *t*-DPPO and a final activity of ~10,000 cpm per μl. A working stock of JH substrate was prepared, using the method of Hammock and Roe (1985), by diluting [^{3}H]-JH III with unlabeled JH III in DMF for a final concentration of 5 mM JH III and a final activity of ~10,000 cpm per μl. Protein concentrations were determined using the BCA assay in a 96-well microplate with BSA as a standard.

2.5. Enzyme assays

Epoxide hydrolase assays with *t*-DPPO were conducted as described previously (Borhan et al., 1995). JHEH microsomes were diluted (100 μl final volume) in 100 mM Tris–HCl, pH 9, containing 0.1 mg ml^{-1} BSA in borosilicate tubes (10 × 75 mm). Typically, 1.8 mU per tube resulted in hydrolysis within the linear range. A unit (U) is defined as the amount of enzyme that will hydrolyze 1 μmol of substrate per min. Substrate (1 μl) was added to each tube, the contents were mixed and the tubes were incubated in a 30 °C shaking water bath. Methanol (60 μl) and isooctane (250 μl) were added to the reaction mixture after transfer to an ice bath then vortexed vigorously until an emulsion was formed. Following centrifugation for 5 min at 3000 rpm (1000***g***), 40 μl of the aqueous bottom phase was counted in 1 ml of Cytoscint using a Wallac 1409 Liquid Scintillation Counter (Gaithersburg, MD). In inhibition screens, prospective inhibitors (1 μl in DMF) were added to assay tubes containing enzyme and preincubated for 10 min at 30 °C prior to addition of substrate. The preincubation period was primarily for convenience to accommodate the screening of multiple inhibitors. Time course assays, in which preincubation times were varied, indicated that inhibitory potency was not affected by duration of exposure of enzyme to inhibitor prior to substrate addition. Partition assays for JHEH activity upon JH III were performed as described in Mumby and Hammock (1979). Neither BSA concentration (from 0 to 5 mg ml^{-1} BSA) nor addition of heat-inactivated microsomes had an effect on IC_{50} values determined in assay validation experiments. Microsomes had no esterase activity acting on JH III as indicated by TLC analysis. Moreover, microsomes prepared from *T. ni* Hi-5 cells infected by a *lacZ* recombinant baculovirus (Debernard et al., 1998) contained no activity on JH III; therefore, all JHEH activity is due to the recombinant JHEH from *M. sexta*.

2.6. Linear range of enzyme activity

The linear range of enzyme activity was determined for both time and enzyme concentration. Microsome samples were prepared for assay by serial dilution and were incubated with substrate for 10 (*t*-DPPO) or 15 min (JH III). Subsequently, a time course of hydrolysis was done at a single dilution, chosen from dilution experiment results, to determine the linear range for incubation times.

2.7. K_m and V_{max} determination

Final substrate concentrations for K_m and V_{max} assays were 10, 25, 50, 75, 100, 150, 200, 300, and 500 μM for *t*-DPPO, and 0.6, 1.3, 2.5, 5, 7.5, 10, and 15 μM for JH III. Assays were run as described above using

conditions within the linear range. K_m and V_{max} were calculated by nonlinear regression using SigmaPlot v. 4 (SPSS, Inc.) to fit the function $f(x) = (V_{max} * x)/(K_m + x)$, where x = concentration of substrate, to the data from enzyme assays expressed as nmol min^{-1}.

2.8. In vitro determination of inhibitory potency

IC_{50}s were determined by linear regression of percent inhibition of *t*-DPPO hydrolysis plotted versus the log of the concentration of inhibitor used. A single IC_{50} experiment consisted of five inhibitor concentrations, assayed in triplicate, which were chosen within the linear region of the inhibition curve so that at least two were above and two below the concentration inhibiting 50% of hydrolysis. Standard deviations of enzyme activities among inhibitor concentration replicates were less than 10% of the average. All IC_{50}s reported are averages of values determined in three separate experiments. In all cases the inhibited enzyme activities were compared to the activity of enzymes exposed to solvent alone. Chemicals were generally stable following dilution so that IC_{50} assays yielded similar values from day to day, except in the case of carbamates and carbodiimide, for which IC_{50}s increased over time, thus the compounds were diluted immediately prior to assay.

2.9. Molar refractivity calculations

Molar refractivity values were calculated using ChemOffice Ultra 2000 (CambridgeSoft Corporation, Cambridge, MA). The parameter indicates the size and polarizability of a chemical and is frequently used in defining quantitative structure-activity relationships to predict effective substrates or inhibitors of enzyme function.

3. Results

3.1. Linear range of assay

Enzyme dilutions and times of incubation were assayed to ensure that substrate remained at saturating concentrations. JHEH constitutes approximately 26% of microsomal protein, according to SDS–PAGE analysis (data not shown). Masses plotted correspond to those of the crude microsomal extracts used in the assays. JH hydrolysis remained linear with concentrations of crude microsomes from 4 to 30 μg ml^{-1} with 15 min of incubation (Fig. 1A). JH hydrolysis remained linear at 20 μg ml^{-1} and time varied from 30 s to 12 min (Fig. 1B). Varying dilution and incubating 10 min (Fig. 2A) indicated a linear range of *t*-DPPO hydrolysis between 6 and 100 μg ml^{-1} crude microsomal dilutions. Varying time of incubation at 100 μg ml^{-1} (Fig. 2B), indicated a linear range of *t*-DPPO hydrolysis between 15 s and 10 min of incubation. Hydrolysis of *t*-DPPO and JH III remained linear over time and with dilution until approximately 35 and 40% of substrate was hydrolyzed, respectively. Above these percentages, the relationship between hydrolysis and enzyme concentration or time of incubation reached a plateau. During enzyme assays, as the number of units of enzyme or duration of incubation increased, substrate hydrolysis reached an apparent maximum when 50% of the substrate was hydrolyzed. In subsequent assays, enzyme concentrations and incubation times were chosen so that 35% hydrolysis or less occurred; these conditions were considered within the linear range of the assay.

3.2. Kinetic constants

Partition assays were performed with varied substrate concentrations to determine the K_m and V_{max} of the substrate for the enzyme. Fig. 3 displays the saturation curve of JHEH hydrolysis of JH III by 0.6 μg crude microsomal extract. Nonlinear regression yielded a K_m value of 3.6 μM and a V_{max} of 322 nmol min^{-1} mg^{-1} for JH III. Fig. 4 shows the saturation curve of JHEH hydrolysis of *t*-DPPO. Nonlinear regression using SigmaPlot yielded a K_m value of 65.6 μM and a V_{max} of 59 nmol min^{-1} mg^{-1}. Thus, the K_m of JHEH for JH III is 18 times lower than for *t*-DPPO, and the V_{max} is 5.5-fold greater for JH III. Previous studies demonstrated that *t*-DPPO diol and JH diol are the only products produced by the recombinant enzyme from *t*-DPPO and JH III.

3.3. IC_{50} assays

t-DPPO was chosen as a surrogate substrate for JHEH. Assays with JH III indicated that the ureas inhibited JH hydrolysis poorly (32% inhibition at 500 μM inhibitor concentration for the N-[(Z)-9-octadecenyl]-N′-propylurea). Previous experiments comparing JHEH activity on multiple epoxide-containing substrates indicated that *t*-DPPO was the best available alternative substrate (Debernard et al., 1998).

Initial screening assays were conducted to determine which structural features led to improved inhibitory potency. Table 1 includes results from a subset of these assays which were the most illuminating. Ureas can have up to four N-substituents with many combinations possible. The compounds presented differ by number, identity and location of substitutions, as well as by size of the inhibitor molecule. Compounds **1–4** are ureas with small substituents in varied locations. These compounds are capable of little hydrophobic bonding with regions adjacent to the active site and do not inhibit even at high concentrations. Compounds **4–6** contain six non-pharmacophore carbon atoms and differ with respect to connectivity to the urea pharmacophore. Only **5** demon-

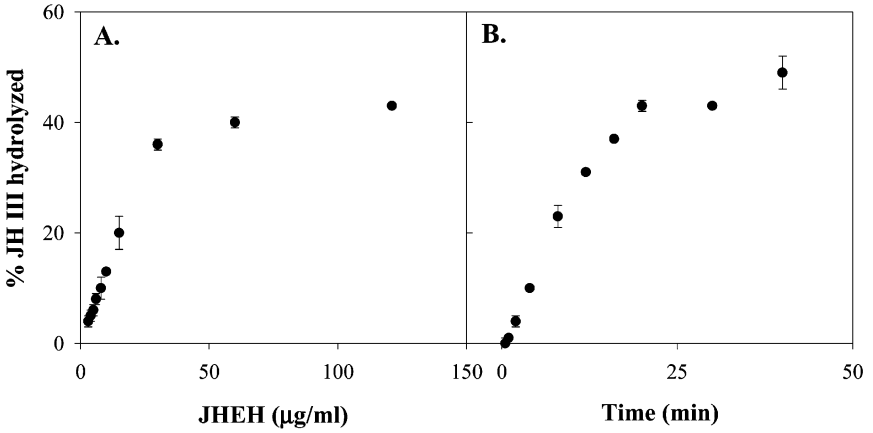

Fig. 1. Effect of enzyme concentration and incubation time on JHEH hydrolysis of a putative natural substrate, [^{3}H]-juvenile hormone III (50 μM). (A) Substrate was incubated with varied JHEH concentrations for 15 min. (B) Substrate was incubated for varied times at a single concentration (0.02 mg ml^{-1}). JHEH was diluted in 100 μl Tris–HCl (100 mM; pH 9) containing 0.1 mg ml^{-1} BSA and incubated at 30 °C. JH III diol and JH III were partitioned by adding 100 μl of methanol, emulsifying with 250 μl of isooctane and centrifuging at ~2000***g***. Data are means of three replicate tubes handled concurrently and represent the percentage of available JH converted to JH diol.

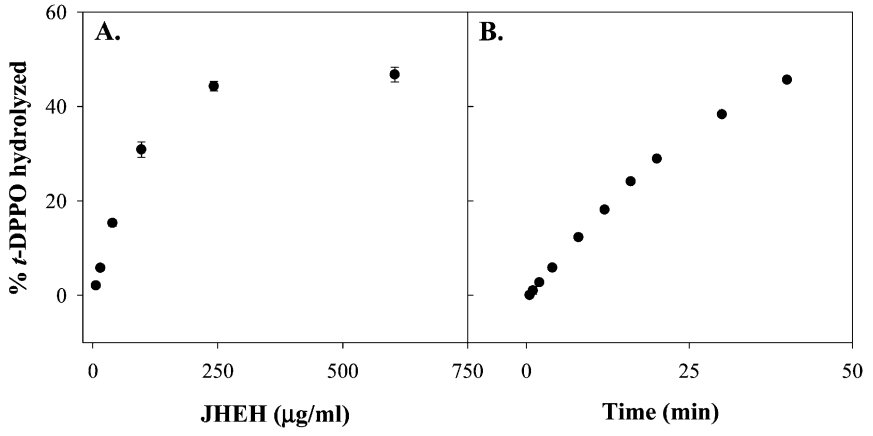

Fig. 2. Effect of enzyme concentration and incubation time on JHEH hydrolysis of the surrogate substrate [^{3}H]-*trans*-diphenylpropene oxide (50 μM). (A) Substrate was incubated with varied JHEH concentrations for 10 min. (B) Substrate was incubated for varied times at a single concentration of crude microsomes (75-fold dilution; 0.04 mg ml^{-1}). Assay conditions are similar to those described for the JH III partition assay in Materials and Methods and Fig. 1, with the exception of addition of 60 μl of methanol in extraction procedure. Standard deviations are shown in both (A) and (B).

strates any inhibitory capability, indicating that substitution of both nitrogen atoms is necessary. Comparison of the inhibitory potencies of **6** and **7** underscores the importance of N, N′-disubstitution. The disubstituted N, N′-dicyclohexylurea (**7**) has a 15-fold lower IC_{50} than **6** which is monosubstituted. While the dicyclohexylurea (**7**) has a fair inhibitory potency, replacing one or both cyclic six-membered substituents with six-membered planar aromatic rings as in N-cyclohexyl-N′-phenylurea or N, N′-diphenylurea (**8** and **9**, respectively) increases the IC_{50} by at least 15-fold. However, in assays comparing percent inhibition at a single concentration by **7–9**, N-cyclohexyl-N′-phenylurea exhibits an intermediate level of inhibition of JHEH activity with respect to the dicyclohexyl and diphenyl compounds (data not shown). Compounds **8** and **10–13** were assayed to explore the effect of placing an alkyl linker of varied length between the urea pharmacophore and the phenyl substituent. Ureas **10–13** contain one, two, three and four-membered alkyl groups, respectively, between the urea pharmacophore and the benzene ring. Compound **8** has no intervening carbon atoms between the urea and the benzene ring and has an IC_{50} of >500 μM. Adding a single carbon atom between the urea and benzene as in **10** reduces the IC_{50} at least 18-fold. The IC_{50} becomes higher (**11**) when an ethylene group is inserted, but each additional carbon atom inserted (**12** and **13**) leads to 19 and 45 times improvement over **8**, respectively. Compounds **14** and **15** are stereoisomers containing a single intervening carbon atom to which a methyl group is bonded. JHEH is apparently enantioselective, with a 2.5-fold higher preference for the R isomer (**14**) over the S

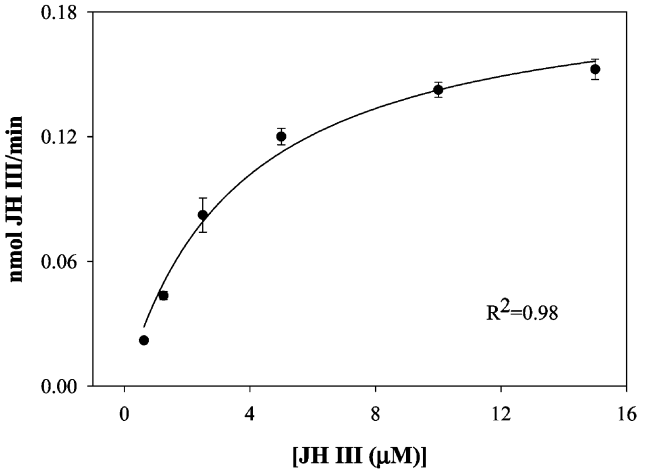

Fig. 3. JHEH hydrolysis of [^{3}H]-juvenile hormone III: Saturation curve represents data from partition assays of JHEH activity on increasing concentrations of JH III (1 μl of substrate in 100 μl assay; 0.63, 1.3, 2.5, 5.0, 10, 15 μM final concentration). Each datum point represents an average of triplicate samples run in parallel. The R^2 for nonlinear regression using SigmaPlot is 0.98.

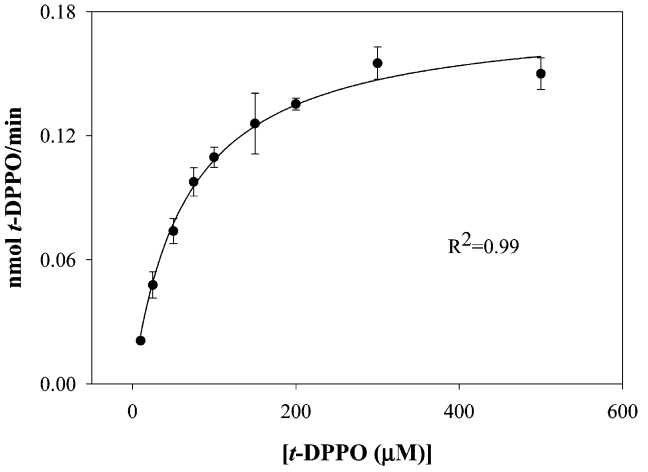

Fig. 4. JHEH hydrolysis of [^{3}H]-*trans*-diphenylpropene oxide: Saturation curve represents data from partition assays of JHEH activity on increasing concentrations of *t*-DPPO (1 μl of substrate in 100 μl assay; 10, 25, 50, 75, 100, 150, 200, 300, 500 μM final concentration). Each datum point represents an average of triplicate samples run in parallel. The R^2 value is 0.99.

isomer (**15**). This is supported in part by the data in Figs. 1 and 2, suggesting that JHEH only hydrates one of the optical isomers of JH III and *t*-DPPO. Replacing the hydrogen atom of compound **10** with a methyl group adjacent to the urea pharmacophore as in **14** and **15**, results in a 3.2 and a 1.3-fold reduction in inhibitory potency, in that order. Based on the N-cyclohexyl-N′-phenyl structure (**8**), a limited number of substituents on the aromatic ring were evaluated. Hydrophobic alkyl groups in the *para* position (**16**, **17**) failed to increase potency dramatically, as did a *para*-chloro atom (**18**). However, a *meta*-chloro substituent in compound **19** increased inhibitory potency.

Various dicyclohexyl compounds were synthesized containing a variety of pharmocophores in order to test whether other pharmacophores would improve inhibitory potencies. IC_{50} assays were conducted to determine the optimal pharmacophore for the JHEH inhibitors (Table 2). All compounds were disubstituted with R=R′=cyclohexyl, to eliminate the possibility that asymmetric substituents were orienting the molecule in the active site, rather than the pharmacophore itself. The IC_{50} data from these assays are presented in rank order, with compound **20** containing the best pharmacophore for JHEH inhibition, and compounds **23** and **24** containing the worst. The urea (**7**) has an IC_{50} which is 2.3 times higher than that of the amide; the carbamate's IC_{50} (**21**) is 6.8 times higher, followed by the IC_{50} of the carbodiimide (**22**) which is 11 times higher. Thiourea (**23**) and thiocarbamate (**24**) both have IC_{50}s approximately 36 times higher than that of the amide.

Since the ureas (**7** and **9**) which contained identical substituents were poor inhibitors compared to those containing asymmetric substituents as in **13** and **19**—a result consistent with asymmetry around the active site of the enzyme—it was considered likely that nonidentical substituents attached to amides would be more potent inhibitors based on positioning of the heteroatom relative to the carbonyl carbon atom. Such compounds have two possible structural isomers, which could interact with varying potencies with the active site of the enzyme. Thus, we compared structural isomers of each of the top three pharmacophores determined above—amides, ureas, and carbamates—to test whether orientation of nonidentical substituents of asymmetric pharmacophores had an effect on inhibitory potency. Alkyl substituents were chosen for these assays since screening indicated that asymmetric N, N′-alkyl substituents led to the greatest potency. The results of these assays are presented in Table 3. Although results with dicyclohexyl-substituted compounds indicated that amide pharmacophores were the most potent, when the best inhibitor from each pharmacophore type (this time substituted with alkyl groups) was compared in **25–27**, the urea (**25**) was the best inhibitor, followed by the amide (**26**; IC_{50} 1.7 times higher) and the carbamate (**27**; IC_{50} at least 2480 times higher than the urea and 1490 times greater than the amide). These data indicate a different order of potency for asymmetrically substituted pharmacophores than for symmetrically substituted ones, with amide and urea groups exchanging rank. Replacement of an amino group within the pharmacophore by either a methylene group (**26**) or oxygen atom (**27**) resulted in reduced inhibitory potency. Replacing the amino hydrogen atom with a methyl group on the shorter side (**28**) resulted in an 8.3-fold increase in IC_{50} compared to the urea, and a 5.0-fold increase compared to the amide. The ideal orientation of amide substitution was for the long alkyl group to be appended to the amide amino group (**29** is less potent

Table 1
The effect of substitutions on IC_{50}s of ureas against hydrolysis of *t*-DPPO by *Ms*JHEH

No	Structure	IC_{50}±SD (μM; $n = 2$)[a]	No	Structure	IC_{50} ±SD (μM; $n = 2$)
1	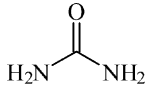	>500[b]	11	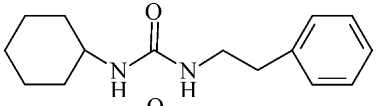	64 ± 1
2	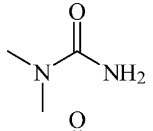	>500	12	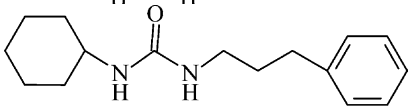	26 ± 1
3	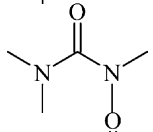	>500	13	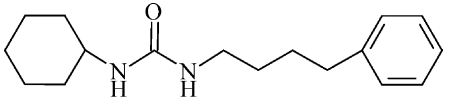	11 ± 2
4	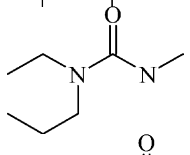	>500	14	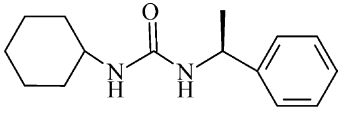	89 ± 4
5	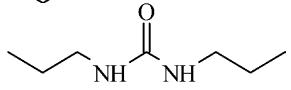	251 ± 7	15	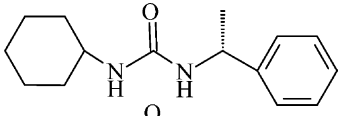	36 ± 4
6	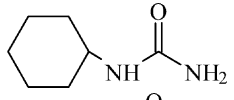	>500	16	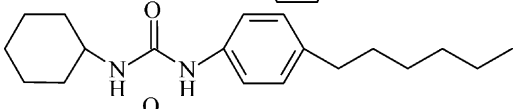	>500
7	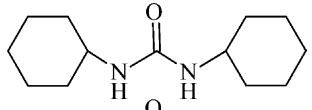	32 ± 1	17	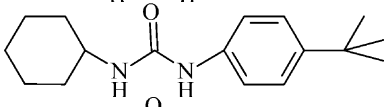	>500
8	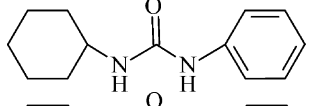	>500	18	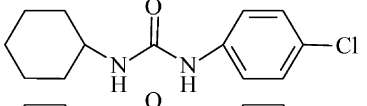	>500
9	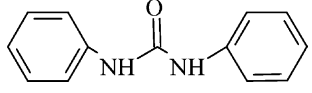	>500	19	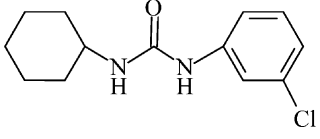	16 ± 0
10	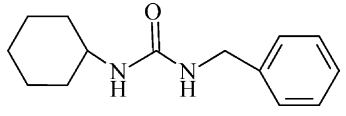	27 ± 0			

[a] IC_{50} refers to the concentration of inhibitor which results in inhibition of 50% of the enzyme activity on *t*-DPPO. The value of *n* refers to the number of assays used to determine the average IC_{50}. Each of the *n* assays consisted of triplicate samples at each concentration assayed, minimally four concentrations with two above and two below the IC_{50}.

[b] Values for IC_{50}s listed as >500 indicate that 50% of enzyme activity was not inhibited even when chemical concentrations of 500 μM were used. Greater concentrations were not assayed because these compounds were considered poor inhibitors of JHEH.

Table 2
The effect of pharmacophores with symmetric substitutions on IC_{50}s against hydrolysis of *t*-DPPO by *Ms*JHEH

No	Structure	Pharmacophore	IC_{50}± SD (μM; $n = 3$)[a]
20	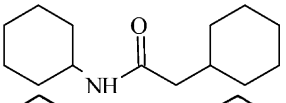	Amide	14.0 ± 0.4
7	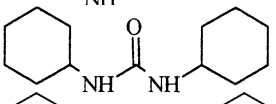	Urea	31.8 ± 1.4
21	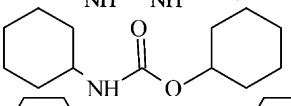	Carbamate	95.1 ± 6.1
22	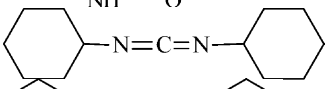	Carbodimide	154 ± 6
23	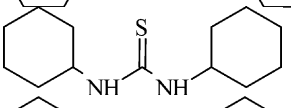	Thiourea	>500[b]
24	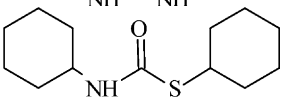	Thiocarbmate	>500

[a] See Table 1 footnote a.
[b] See Table 1 footnote b.

Table 3
The effect of orientation of pharmacophores with asymmetric substitutions on IC_{50}s against hydrolysis of *t*-DPPO by *Ms*JHEH

No	Structure	IC_{50} ±SD (μM; $n = 3$)[a]
25	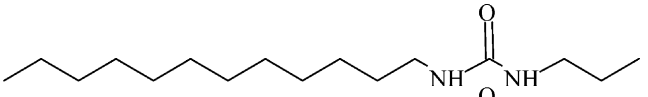	0.18 ± 0.05
26	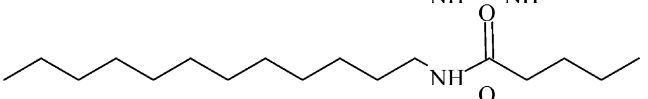	0.30 ± 0.04
27	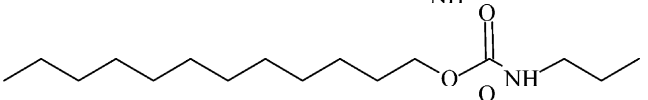	447 ± 43
28	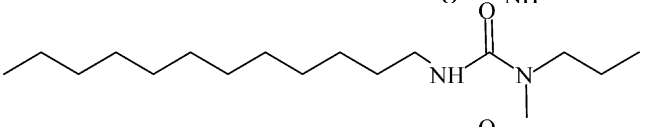	1.49 ± 0.14
29	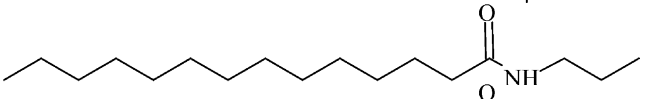	1.91 ± 0.09
30	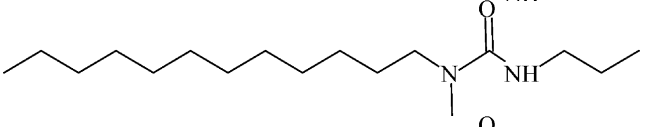	2.26 ± 0.15
31	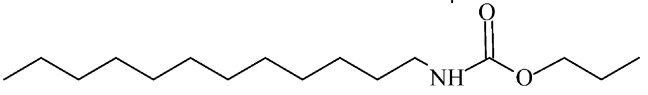	>500[b]

[a] See Table 1 footnote a.
[b] See Table 1 footnote b.

than **26**). The importance of having the long alkyl side adjacent to the amino group was again supported by comparison of **30** and **28**, in which moving the methyl substituent from the long to the short alkyl side resulted in a 1.5-fold improvement in potency. The improvement in potency was not due to the presence of a methyl substituent on the amino group on the small side, as indicated by comparison of **28** and **25** in which addition of the methyl group in that location gave an 8.3-fold loss of potency. Apparently, the improved potency of **28** compared to **30** was due to the restoration of a hydrogen atom on the side of the long alkyl group. Neither orientation of asymmetric substituents of carbamates (**27** and **31**) led to potent inhibition of JHEH. Surprisingly, the IC_{50}s were 5.3-fold worse in the carbamates containing nonidentical substituents (**27**, **31**) than in the dicyclohexyl compound (**21**). Thus, the characteristic shared in the three best inhibitors in this series (**25**, **26**, and **28**) was the presence of an amino group on the long alkyl side of the pharmacophore.

To verify that the inhibition of JHEH was not due to amine or amide minor contaminants, a panel of primary amines and amides of varying lengths was assayed against JHEH at one high and one low concentration. These data are presented in Table 4 as percent inhibition measured using the amine and amide inhibitors at 100 and 1 μM concentrations. A high concentration of 100 μM was chosen to determine whether amines and amides were potent at all; a low concentration of 1 μM was chosen, well above the likely concentrations in which amine or amide contaminants would be present, to demonstrate that these compounds are unlikely to contribute substantially to the inhibitory potencies measured. The numbers reported for percent inhibition are averages of two separate determinations using triplicate samples in each assay. All amines and the amide presented in Table 4 were poor inhibitors at low concentrations (**32–42**). Short to moderate length alkyl amines were also poor inhibitors at high concentrations (**32–35**). Inhibition by undecylamine (**36**) was approximately 50% at 100 μM, indicating a fairly high IC_{50}. Amines having an alkyl group length greater than eleven carbon atoms appeared to be more potent (**37–40**), with the greatest percent inhibition by tridecylamine (**38**). Introducing a double bond (**41** vs **40**) increased the potency of octadecylamine. However, comparison of the octadecenylamine (**41**) with the octadecenylamide (**42**) indicates an approximately 2-fold reduction of inhibition under otherwise identical conditions.

As indicated above, ureas constituted the best inhibitors of hydrolysis of *t*-DPPO by JHEH. Experiments were conducted to test the effects of varying alkyl length on IC_{50}. Results are presented in Table 5, in which the short alkyl chain was held constant as propyl (**25**, **43–50**) with inhibitors listed in order of increasing lengths of R; and in Table 6, in which the long alkyl substituent is held constant as dodecyl (**25**, **51–58**) and the short alkyl substituents were varied. The potency increased

Table 4
Percent inhibition of *t*-DPPO hydrolysis by *Ms*JHEH in presence of primary amines and amides

No	Structure	% Inhibition (100 μM)	% Inhibition (1 μM)
32	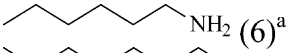	1	1
33	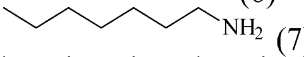	6	2
34	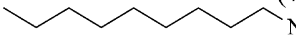	15	3
35	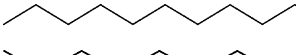	26	0
36	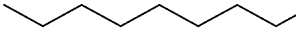	44	6
37	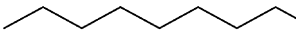	64	2
38	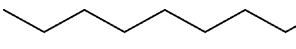	80	4
39	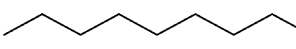	71	3
40	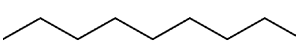	67	4
41	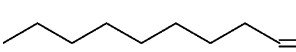	89	2
42	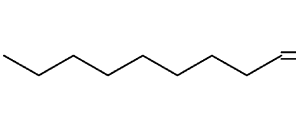	46	2

[a] The numbers in parentheses indicate the number of carbon atoms in the N-alkyl substituents.

Table 5
IC_{50}s of N-propyl ureas with varied long N′-alkyl groups

No	Structure	IC_{50}±SD (μM; $n = 3$)[a]
43	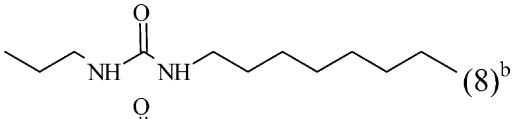 (8)[b]	1.56 ± 0.13
44	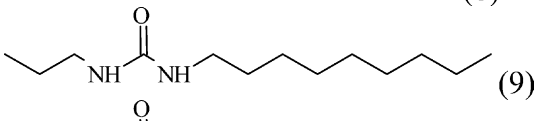 (9)	0.78 ± 0.08
45	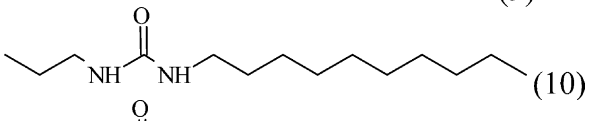 (10)	1.76 ± 0.14
46	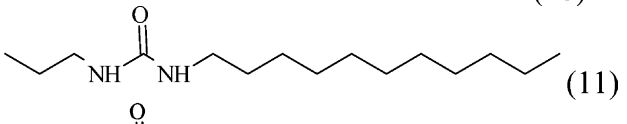 (11)	0.16 ± 0.01
25	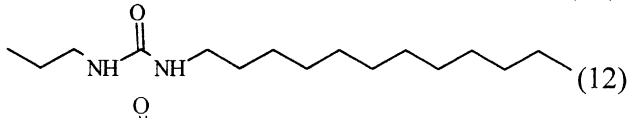 (12)	0.18 ± 0.05
47	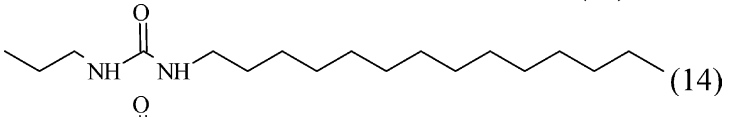 (14)	0.14 ± 0.02
48	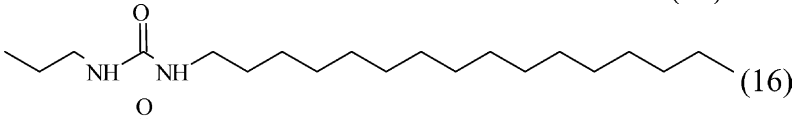 (16)	0.09 ± 0.01
49	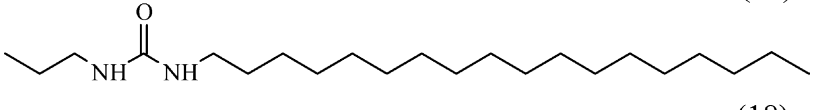 (18)	0.34 ± 0.05
50	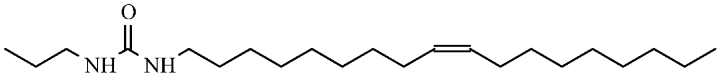 (18, Δ-9,10)	0.08 ± 0.02

[a] See Table 1 footnote a.
[b] See Table 4 footnote a.

with increasing lengths of the longer alkyl chain (Table 5) with the most potent inhibitors being **48** (R: 16 carbon atoms) and **50** (R: 18 carbon atoms, Δ-9,10). Compounds **49** and **50** differ only in the presence of a double bond mid-chain, which appeared to improve the inhibitory potency by about 4.6-fold. In assays to optimize the short alkyl chain length (Table 6), inhibitory potencies were low in the monosubstituted N-dodecylurea (**51**). Placing short, branched or unbranched alkyl groups on the second nitrogen atom improved inhibitory potency (**52–58**). Compounds containing at least three carbon atoms extending linearly from the N′nitrogen atom appeared to have the lowest IC_{50}s (**25**, **54–57**), while those containing no N′-substituent (as in **51),** an N′-ethyl group (as in **52)**, or an N′-isopropyl group (as in **53**) had decreased potencies. When the longest linear chain of carbon atoms in the short alkyl group contained three carbon atoms, branching appeared not to have any major effects on inhibitory potency (**25**, **54**, **55**, **57**). Once the longest linear carbon atom chain extended beyond three, however, potencies began to decrease, with N′-*n*-butyl substitution leading to a modest increase of IC_{50} (**56**), and N′-isoamyl substitution resulting in a marked increase of IC_{50} (**58**).

To investigate the possibility that the inhibitors could be acting nonspecifically, and to investigate the possibility that either the BSA added to the assay or the proteins present along with JHEH in the microsomes could affect the IC_{50}s of the inhibitors by providing hydrophobic regions that could sequester the inhibitors, an experiment was conducted to test the effect of BSA concentrations or addition of heat-inactivated microsomes on IC_{50}s determined for compound **50**. The results are displayed in Table 7. IC_{50}s (1–5) ranged from 0.05 to 0.11 μM for BSA concentrations ranging from 0–5 mg ml^{-1}. When buffer was prepared to contain 0.05 mg ml^{-1} of heat-inactivated microsomes and 0.05 mg ml^{-1} BSA, or a total of 0.1 mg ml^{-1} protein, the IC_{50} value

Table 6
IC_{50}s of N-dodecyl ureas with varied short N′-alkyl groups

No	Structure	IC_{50}±SD (μM; n=3)[a]
51	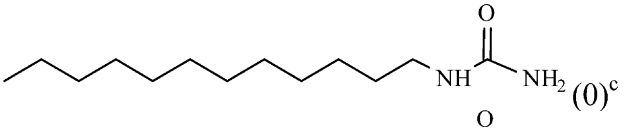 (0)[c]	>500[b]
52	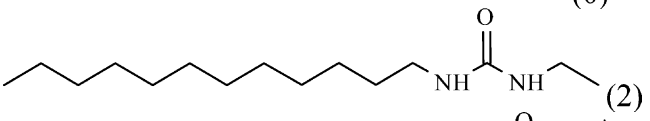 (2)	0.60 ± 0.05
53	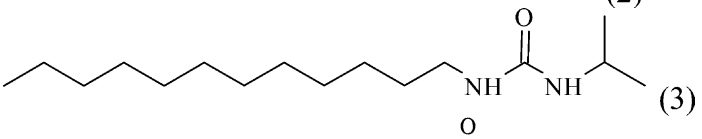 (3)	0.40 ± 0.02
25	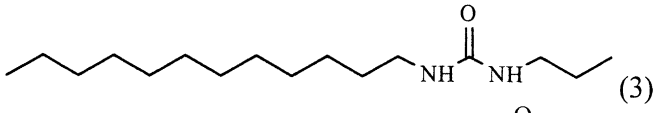 (3)	0.18 ± 0.05
54	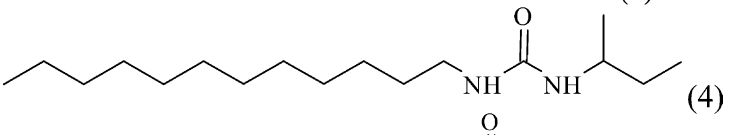 (4)	0.17 ± 0.02
55	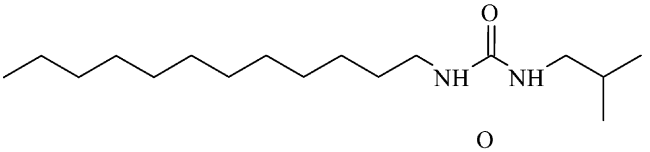 (4)	0.20 ± 0.03
56	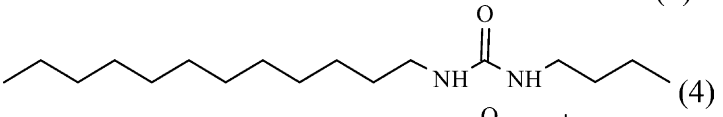 (4)	0.27 ± 0.03
57	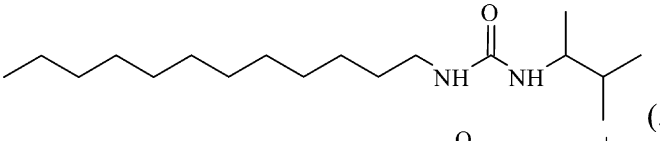 (5)	0.21 ± 0.03
58	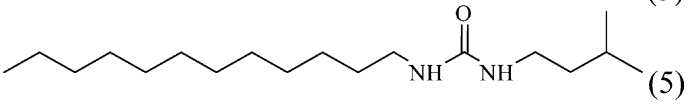 (5)	1.4 ± 0.3

[a] See Table 1 footnote a.
[b] See Table 1 footnote b.
[c] See Table 4 footnote a.

determined was 0.09 μM. The addition of heat-inactivated microsomes also results in a threefold increase in the amount of Triton X-100 in the assay. When the inhibitor was not preincubated with JHEH, the IC_{50} (number 6) fell within the range of the IC_{50} determined following a 10 min preincubation. Each IC_{50} value in Table 7 was determined from a single assay whereas the IC_{50}s reported in Tables 1–6 are averages of three assays. When IC_{50}s reported in Table 7 (1–6) were averaged, the mean of 0.08 μM was the same as that recorded for **50** (see Table 7, number 8).

3.4. Molar refractivities

Molar refractivities of juvenile hormones are displayed in Table 8. Values for molar refractivities reflect the volume occupied by a chemical and are often predictors of quantitative structure-activity relationships between substrates or inhibitors and changes in catalytic activity of target enzymes.

4. Discussion

4.1. JHEH role and inhibition

The enzyme used in this study has been called JHEH. Certainly it hydrolyzes the JH epoxide, but absolute proof that this is the only role or even a physiological role of the enzyme is lacking. Evidence in support of its physiological role in regulating JH titer includes the specificity (k_{cat}/K_m) that the enzyme shows for JH com-

Table 7
Effect of BSA or microsome addition on IC_{50}s

No.	Treatment	Concentration (mg ml^{-1})	IC_{50} (μM)[a]
1	BSA	None	0.06
2		0.05	0.05
3		0.10	0.05
4		1.00	0.10
5		5.00	0.11
6	Microsomes[b]	0.05	0.09
7	No preincubation[c]	0.10	0.06
8	Average of 1–6	–	0.08 ± 0.01
9	Compound 50[d]	0.10	0.08 ± 0.02

[a] Values were determined for a single assay by linear regression of averages of three replicate tubes at three concentrations within the linear region surrounding the IC_{50}. The substrate was *t*-DPPO.

[b] Microsomes were heat inactivated for 10 min at 70 °C prior to addition to buffer containing 0.05 mg ml^{-1} BSA.

[c] All conditions were the same as the standard assay, except that inhibitor and substrate were added to 50 μl of buffer and the assay was started by the addition of 50 μl of enzyme diluted in buffer.

[d] The IC_{50} value is for for N-[(Z)-9-octadecenyl]-N′-propylurea (compound 50 in Table 5) on *Ms*JHEH using *t*-DPPO for a substrate.

Table 8
Structures and molar refractivities of the juvenile hormones

No	Structure	MR (cm^3 mol^{-1})[a]
59	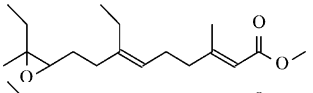	87.58
60	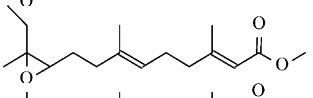	82.98
61	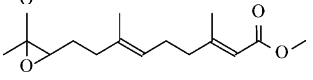	78.46

[a] MR is an abbreviation for molar refractivity.

pared to the other substrate in this study and in those assayed by Touhara and Prestwich (1993). The correlation of its presence with endocrine events and the formation of JH diol and subsequent metabolites supports the hypothesis (Halarnkar and Schooley, 1990). The similarity of structure of the most potent inhibitors in both the glycidol series (Linderman et al., 2000) tested on the homologous enzyme from *T. ni*, and in this study, also support the hypothesis. However, neither series of inhibitors are potent enough yet to eliminate the activity of the enzyme in vivo and test directly the role of JHEH in endocrine regulation.

Linderman et al. (2000) reported potent inhibitors of the JHEH of *T. ni* based on the glycidol structure. On analogy to the inhibition of the mammalian sEH by glycidols (Dietze et al., 1991) and the similar chalcone oxides (Morisseau et al., 1998; Mullin and Hammock, 1982), one can anticipate that they are kinetically irreversible inhibitors which are slowly turned over by the enzyme. Because of this turnover and because of the potential instability of the parent compounds in the presence of glutathione S-transferase, by analogy with chalcone oxides (Miyamoto et al., 1987), a search for potent, stable and kinetically reversible inhibitors of the mammalian enzyme was undertaken. The study resulted in the urea, carbamate and amide series applied to JHEH in this paper. Several urea inhibitors have been crystallized with the mammalian soluble epoxide hydrolase (Argiriadi et al., 2000; Argiriadi et al., 1999). Based on analogy with the mammalian enzyme, we hypothesize that the inhibitors introduced in this manuscript are acting as transition state mimics with the insect enzyme (Fig. 5).

4.2. Proposed model of inhibition

Based on the alignment and conservation of the amino acid residues Asp227, His428, Glu404, Tyr298, and Tyr372 in the JHEH of *M. sexta* (Q25489) as compared to microsomal EHs (all accession numbers in parentheses are from the SwissProt/TrEMBL database) from *T. ni* (O44124, Q94806), *D. melanogaster* (Q9V8P3), *Rattus norvegicus* (P07687), and *Homo sapiens* (P07099), as well as structural information from the EH

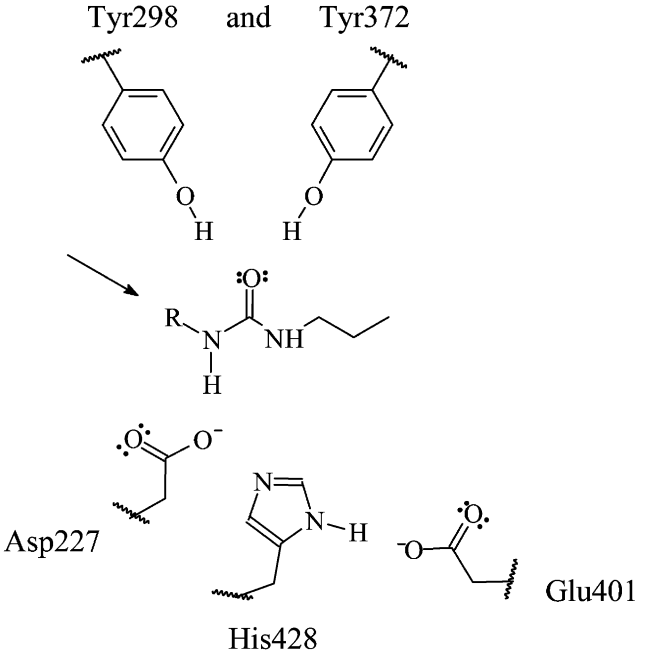

Fig. 5. Schematic representation of the interaction of JHEH with a urea inhibitor. The N-[(Z)-9- octadecenyl]-N′-propylurea is indicated with an arrow. The structures correspond to the side chains of amino acids in the primary sequence of the JHEH of *M. sexta* which align with amino acids implicated in catalysis by the mEH of *R. norvegicus* and *H. sapiens* (SwissProt accession numbers Q25489 and P07687, respectively). The numbers correspond to amino acids derived from the cDNA sequence of the JHEH of *M. sexta* (Wojtasek and Prestwich, 1996).

of *Aspergillus niger* (Zou et al., 2000) and the sEH of *Mus musculus* (Argiriadi et al., 2000; Armstrong, 1999; Armstrong and Cassidy, 2000, for review of EH structure and mechanism), we propose the model of inhibition presented in Fig. 5. The evidence suggests that epoxide substrates are oriented in the active site through interactions with two tyrosines present in a cap-like domain, and which are part of an 'oxyanion hole'. The substrate, on entry into the active site, undergoes nucleophilic attack by a conserved aspartate. Release of the substrate as a diol occurs after a charge-relay component consisting of histidine and glutamate (or in some cases a second aspartate) activates water which then attacks the carbonyl group of the aspartate, thus breaking the covalent bond between aspartate and the substrate, releasing the diol product, and restoring a kinetically competent enzyme. When the inhibitor enters the active site, the carbonyl group of the urea can interact with the two tyrosines of the oxyanion hole. Having no epoxide present, the compounds do not serve as a substrate for the enzyme, and are not capable of covalent binding to Asp227 of the epoxide hydrolase. We have demonstrated that a nitrogen atom bound to a hydrogen atom and present on the long side of an asymmetric urea is favored. In the diagram, the hydrogen atom is shown extending from the nitrogen atom to distinguish it from the less crucial NH group.

4.3. Linear range of assay

The apparent limit of 50% hydrolysis of *t*-DPPO and JH III substrates in each of the linear range experiments is consistent with stereoselectivity of JHEH for hydrolysis of its substrates. Both *t*-DPPO and JH III are racemic mixtures. Williamson et al. (2000) have shown that the mammalian and plant cytosolic epoxide hydrolases studied have varying enantioselectivities for substrates tested, thus the apparent selectivity of JHEH for its substrates is not surprising.

4.4. K_m of substrates

The K_m of JHEH (3.6 μM) for JH III reported here differs from the K_m of 0.28 μM reported by Touhara and Prestwich (1993). Several factors may contribute to the approximately 13-fold difference in values. First, the substrate used by Touhara was a single isomer, while the substrate used in this work was racemic. Since K_m corresponds to the concentration of substrate required to reach half the maximal rate of hydrolysis, and the presence of the nonbiological racemate would decrease the effective concentration of the natural substrate, a larger concentration of the racemic mixture than the optically active compound would be required to reach 1/2 V_{max} and would thus increase the apparent K_m. Second, the JHEH used in the earlier paper was purified, while our work has used a microsomal extract. Other membrane-bound proteins are undoubtedly enriched in the microsomal fraction along with JHEH, which would provide additional hydrophobic regions for JH to bind non-specifically. Third, Triton X-100 was used to solubilize the microsomal extract at a concentration above its critical micelle concentration, thus JH would be partially sequestered into detergent micelles (Kramer et al., 1974). According to the purification scheme of Touhara and Prestwich (1993), Triton X-100 was removed. The K_m of JHEH for *t*-DPPO and JH III in the current study differ from each other in the manner expected. A considerably higher concentration of *t*-DPPO than JH III (18-fold) is required to attain 1/2 V_{max}. Our strategy in screening inhibitors was to use a non-optimal substrate which should be competitively displaced more easily than the assumed natural substrate.

McGovern et al. (2002) revealed that a series of lipophilic chemicals, appearing as leads from screening for inhibitors with multiple enzymes, were nonspecifically inhibiting enzymes by forming aggregates similar to detergents. These 'promiscuous' inhibitors were time-dependent, presumably because of the time required for aggregate formation, and sensitive to the presence of BSA at 0.1 mg ml^{-1}, which led to a 4- to 50-fold

increase in IC_{50}. To test the hypothesis that the Inhibition of *M. sexta* JHEH inhibitors might be functioning in a manner consistent with aggregate formation, we selected one of the best inhibitors for IC_{50} assays at different concentrations of BSA. There was no dramatic effect on IC_{50} values when BSA concentrations were varied from 0 to 5 mg ml^{-1} or when heat inactivated microsomes were added. The IC_{50} did not change when enzyme was exposed to inhibitor and substrate simultaneously, rather than preincubated with inhibitor, indicating that inhibition was instantaneous. The fact that addition of heat-inactivated microsomes did not have an effect on IC_{50}, in spite of the three-fold increase in Triton X-100 in the assay, provides further support for the validity of the assay and for the compounds being true inhibitors of JHEH activity.

4.5. Characteristics of the most potent inhibitors

While primary amines and amides were optimal inhibitors for the rat and human microsomal epoxide hydrolases (Morisseau et al., 2001), the JHEH of *M. sexta* was poorly inhibited by these compounds (Table 4). These results seem to indicate the presence of two hydrophobic pockets, one small and one relatively larger, on either side of the catalytic site of JHEH. The enzymes were similar, however, in their greater inhibition by compounds containing long alkyl groups.

Although one might expect optimal inhibitors of JHEH to have a molar refractivity approximating that of the juvenile hormones (Table 8), long linear alkyl groups having much larger molar refractivities (**48** and **50**; MR >100 cm^3 mol^{-1}) than JH I, II, and III (**59–61**) were the best inhibitors. Of course, one is comparing linear alkyl inhibitors with branched chain, epoxy methyl farnesoate and homofarnesoate analogs of JH. One must also remain open to the possibility that the enzyme which has been called JHEH may have a function other than JH hydrolysis.

Although assay of symmetrical cyclohexyl compounds differing with respect to pharmacophore indicated a rank order of potencies of amide>urea>carbamate, it is important to note that in later assays using asymmetric linear compounds, the ordering of inhibitory potencies switched to urea>amide>carbamate. Branching on both sides of the pharmacophore, as in the dicyclohexyl compounds, may interfere with close associations of catalytic residues with the nitrogen atoms of amide and urea pharmacophores, and may have shielded them from interacting with the carbamate oxygen atom. This shielding may explain the poorer inhibition by dicyclohexyl amides and ureas and the greater inhibition by dicyclohexyl carbamates than by carbamates in the more accessible linear alkyl compounds.

Recent work in this lab has demonstrated the utility of amide, carbamate and urea inhibitors of mammalian microsomal EHs (Morisseau et al., 2001). Several of these compounds were used in crystallization of the soluble epoxide hydrolase from *M. musculus* and refinement of its crystal structure (Argiriadi et al., 1999, 2000). Moreover, in a spontaneously hypertensive rat model, these compounds have restored normal blood pressure following injection, indicating a potential for use in vivo (Yu et al., 2000). These demonstrations of the utility of ureas and amides to understand the role of epoxide hydrolases in mammalian systems made the extension of these classes of compounds to study the role of JHEH in insect physiology attractive.

This paper presents in vitro optimization of amide, carbamate and urea inhibitors for a microsomal epoxide hydrolase selective for juvenile hormone, and further characterization of the recombinant JHEH of *M. sexta*. While the inhibitory potencies of the urea, amide and carbamate compounds reported are not as high with the *Ms*JHEH as those of glycidol compounds reported on an EH of *T. ni* (Linderman et al., 2000), the compounds have been effective tools to demonstrate important characteristics of inhibitors of *Ms*JHEH. Maximal efficacy is reached with long lipophilic aliphatic compounds, with or without a double bond in mid-chain. While these compounds are effective inhibitors of hydrolysis of *t*-DPPO, inhibition of JH III hydrolysis is in the mid-micromolar range, lending further support for JH as the native substrate for JHEH. Therefore, the compounds described above represent a first generation of stable JHEH inhibitors.

Acknowledgements

This work was supported in part by the USDA Competitive Research Grants Program 97-35302-4406 and 2001-35302-09919, by NIEHS R01 ES02710, NIEHS Superfund Basic Research Program ES04699, and NIEHS Center for Environmental Health Sciences Grant 1P30- ES05707. TFS was supported in part by the UC-Davis Biotechnology Program and by the NIHNIGMS grant #GM08343. The authors are grateful to C. E. Wheelock, J. W. Newman, and T. Watanabe (UC-Davis) for their assistance in acquisition of NMR and MS spectra, and to A. Daniel Jones (Pennsylvania State University) for APCI-MS analysis.

References

Argiriadi, M.A., Morisseau, C., Goodrow, M.H., Dowdy, D.L., Hammock, B.D., Christianson, D.W., 2000. Binding of alkylurea inhibitors to epoxide hydrolase implicates active site tyrosines in substrate activation. J. Biol. Chem. 275, 15265–15270.

Argiriadi, M.A., Morisseau, C., Hammock, B.D., Christianson, D.W., 1999. Detoxification environmental mutagens and carcinogens:

structure, mechanism, and evolution of liver epoxide hydrolase. Proc. Natl Acad. Sci. USA 96, 10637–10642.

Armstrong, R.N., 1999. Kinetic and chemical mechanism of epoxide hydrolase. Drug Metab. Rev. 31, 71–86.

Armstrong, R.N., Cassidy, C.S., 2000. New structural and chemical insight into the catalytic mechanism of epoxide hydrolases. Drug. Metab. Rev. 32, 327–338.

Borhan, B., Mebrahtu, T., Nazarian, S., Kurth, M.J., Hammock, B.D., 1995. Improved radiolabeled substrates for soluble epoxide hydrolases. Anal. Biochem. 231, 188–200.

Brooks, G.T., 1973. Insect epoxide hydrase inhibition by juvenile hormone analogues and metabolic inhibitors. Nature 245, 382–384.

Campbell, P.M., Healy, M.J., Oakeshott, J.G., 1992. Characterization of juvenile hormone esterase in *Drosophila melanogaster*. Insect Biochem. Mol. Biol. 22, 665–677.

Casas, J., Harshman, L.G., Hammock, B.D., 1991a. Epoxide hydrolase activity on juvenile hormone in *Manduca sexta*. Insect Biochem. 21, 17–26.

Casas, J., Harshman, L.G., Messeguer, A., Kuwano, E., Hammock, B.D., 1991b. In vitro metabolism of juvenile hormone III and juvenile hormone III bisepoxide by *Drosophila melanogaster* and mammalian cytosolic epoxide hydrolase. Arch. Biochem. Biophys. 286, 153–158.

De Kort, C.A.D., Granger, N.A., 1981. Regulation of the juvenile hormone titer. Ann. Rev. Entomol. 26, 1–28.

De Kort, C.A.D., Granger, N.A., 1996. Regulation of JH titers: the relevance of degradative enzymes and binding proteins. Arch. Insect Biochem. Physiol. 33, 1–26.

Debernard, S., Morisseau, C., Severson, T.F., Feng, L., Wojtasek, H., Prestwich, G.D., Hammock, B.D., 1998. Expression and characterization of the recombinant juvenile hormone epoxide hydrolase (JHEH) from *Manduca sexta*. Insect Biochem. Mol. Biol. 28, 409–419.

Dietze, E.C., Kuwano, E., Casas, J., 1991. Inhibition of cytosolic epoxide hydrolase by *trans*-3-phenylglycidols. Biochem. Pharmacol. 42, 1163–1175.

Halarnkar, P.P., Schooley, D.A., 1990. Reversed-phase liquid chromatographic esparation of juvenile hormone and its metabolites, and its application for an in vivo juvenile hormone catabolism study in *Manduca sexta*. Anal. Biochem. 188, 394–397.

Hammock, B.D., 1985. Regulation of juvenile hormone titer: degradation. In: Kerkut, G.A., Gilbert, L.I. (Eds.), Comprehensive Insect Physiology, Biochemistry and Pharmacology. Pergamon Press, Oxford, pp. 431–472.

Hammock, B.D., Mumby, S.M., Lee, P.W., 1977. Mechanisms of resistance to the juvenoid methoprene in the house fly *Musca domestica* L. Pestic. Biochem. Phys. 7, 261–272.

Hammock, B.D., Nowock, J., Goodman, W., Stamoudis, V., Gilbert, L.I., 1975. The influence of hemolymph-binding protein on juvenile hormone stability and distribution in *Manduca sexta* fat body and imaginal discs in vivo. Mol. Cell Endocrinol. 3, 167–184.

Hammock, B.D., Roe, R.M., 1985. Analysis of juvenile hormone esterase activity. In: Law, J.H., Rilling, H.C. (Eds.), Methods in Enzymology: Steroids and Isoprenoids. Academic Press, New York, pp. 487–494.

Jesudason, P., Anspaugh, D.D., Roe, R.M., 1992. Juvenile hormone metabolism in the plasma, integument, midgut, fat body, and brain during the last instar of the tobacco hornworm, *Manduca sexta*. Arch. Insect Biochem. Physiol. 20, 87–105.

Kramer, K.J., Sanburg, L.L., Kezdy, F.J., Law, J.H., 1974. The juvenile hormone binding protein in the hemolymph of *Manduca sexta* Johannson (Lepidoptera: Sphingidae). Proc. Natl Acad. Sci. USA 71, 493–497.

Lassiter, M.T., Apperson, C.S., Roe, R.M., 1995. Juvenile hormone metabolism during the fourth stadium and pupal stage of the southern house mosquito, *Culex quinquefasciatus* Say. J. Insect Physiol. 41, 869–876.

Linderman, R.J., Roe, R.M., Harris, S.V., Thompson, D.M., 2000. Inhibition of insect juvenile hormone epoxide hydrolase: asymmetric synthesis and assay of glycidol-ester and epoxyester inhibitors of *Trichoplusia ni* epoxide hydrolase. Insect Biochem. Mol. Biol. 30, 767–774.

McGovern, S.L., Caselli, E., Grigorieff, N., Shoichet, B.K., 2002. A common mechanism underlying promiscuous inhibitors from virtual and high-throughput screening. J. Med. Chem. 45, 1712–1722.

Miyamoto, T., Silva, M., Hammock, B.D., 1987. Inhibition of epoxide hydrolases and glutathione *S*-transferases by 2-, 3-, and 4-substituted derivatives of 4′-phenylchalcone and its oxide. Arch. Biochem. Biophys. 254, 203–213.

Morisseau, C., Du, G., Newman, J.W., Hammock, B.D., 1998. Mechanism of mammalian soluble epoxide hydrolase inhibition by chalcone oxide derivatives. Arch. Biochem. Biophys. 356, 214–228.

Morisseau, C., Newman, J.W., Dowdy, D.L., Goodrow, M.H., Hammock, B.D., 2001. Inhibition of microsomal epoxide hydrolases by ureas, amides and amines. Chem. Res. Toxicol 14, 409–415.

Morisseau, C.H., Goodrow, M.H., Dowdy, D., Zheng, J., Greene, J.F., Sanborn, J.R., Hammock, B.D., 1999. Potent urea and carbamate inhibitors of soluble epoxide hydrolases. Proc. Natl Acad. Sci. USA 96, 8849–8854.

Mullin, C.A., Hammock, B.D., 1982. Chalcone oxides--potent selective inhibitors of cytosolic epoxide hydrolase. Arch. Biochem. Biophys. 216, 423–439.

Mumby, S.M., Hammock, B.D., 1979. A partition assay for epoxide hydrases acting on insect juvenile hormone and an epoxide-containing juvenoid. Anal. Biochem. 92, 16–21.

Nijhout, H.F., 1994. Insect Hormones. Princeton University Press, Princeton, NJ.

Share, M.R., Venkatesh, K., Jesudason, P., Roe, R.M., 1988. Juvenile hormone metabolism during embryogenesis in the tobacco hornworm *Manduca sexta* (L.). Arch. Insect Biochem. Physiol. 8, 173–186.

Slade, M., Brooks, G.T., Hetnarski, H.K., Wilkinson, C.F., 1975. Inhibition of the enzymatic hydration of the epoxide HEOM in insects. Pestic. Biochem. Physiol. 5, 35–46.

Slade, M., Zibitt, C.H., 1971. Metabolism of *Cecropia* juvenile hormone in Lepidopterans. In: Tahori, A.S. (Ed.), Chemical Releases in Insects. Gordon & Breach, pp. 45–58.

Slade, M., Zibitt, C.H., 1972. Metabolism of *Cecropia* juvenile hormone in insects and in mammals. In: Menn, J.J., Beroza, M. (Eds.), Insect Juvenile Hormones: Chemistry and Action. Academic Press, New York, pp. 155–176.

Sparks, T.C., Hammock, B.D., 1980. Comparative inhibition of the juvenile hormone esterases from *Trichoplusia ni*, *Tenebrio molitor*, *Musca domestica*. Pestic. Biochem. Physiol. 14, 290–302.

Sparks, T.C., Hammock, B.D., Riddiford, L.M., 1983. The haemolymph juvenile hormone esterase of *Manduca sexta* (L.)—inhibition and regulation. Insect Biochem. 13, 529–541.

Touhara, K., Prestwich, G.D., 1993. Juvenile hormone epoxide hydrolase: photoaffinity labeling, purification, and characterization from tobacco hornworm eggs. J. Biol. Chem. 268, 19604–19609.

Williamson, K.C., Morisseau, C., Hammock, B.D., 2000. Regio- and enantioselective hydrolysis of phenyloxiranes catalyzed by soluble epoxide hydrolase. Tetrahedron 11, 4451–4462.

Wing, K.D., Sparks, T.C., Lovell, V.M., Levinson, S.O., Hammock, B.D., 1981. The distribution of juvenile hormone esterase and its interrelationship with other proteins influencing juvenile hormone metabolism in the cabbage looper, *Trichoplusia ni*. Insect Biochem. 11, 473–485.

Wojtasek, H., Prestwich, G.D., 1996. An insect juvenile hormone-specific epoxide hydrolase is related to vertebrate microsomal epoxide hydrolase. Biochem. Biophys. Res. Co. 220, 323–329.

Yamada, T., Morisseau, C., Maxwell, J.E., Argiriadi, M.A., Christianson, D.W., Hammock, B.D., 2000. Biochemical evidence for the

involvement of tyrosine in epoxide activation during the catalytic cycle of epoxide hydrolase. J. Biol. Chem. 275, 23082–23088.

Yu, Z., Xu, F., Huse, L.M., Morisseau, C., Draper, A.J., Newman, J.W., Parker, C., Graham, L., Engler, M.M., Hammock, B.D., et al. 2000. Soluble epoxide hydrolase regulates hydrolysis of vasoactive epoxyeicosatrienoic acids. Circ. Res. 87, 992–998.

Zou, J., Hallberg, B.M., Bergfors, T., Oesch, F., Arand, M., Mowbray, S.L., Jones, T.A., 2000. Structure of *Aspergillus niger* epoxide hydrolase at 1.8 A resolution: implications for the structure and function of the mammalian microsomal class of epoxide hydrolases. Structure 8, 111–122.